Towards a higher photostability of ZnO photo-electrocatalysts in the degradation of organics by using MMO substrates

Lorena A. Goulart[a,d], Géssica O. S. Santos[b,d], Katlin I.B. Eguiluz[b,c], Giancarlo R. Salazar-Banda[b,c], Marcos R. V. Lanza[a,*], Cristina Saez[d], Manuel A. Rodrigo[d,*]

[a] *Institute of Chemistry - São Carlos, University of São Paulo, P.O. Box 780, CEP-13560-970 São Carlos, SP, Brazil.*

[b] *Processes Engineering Post-graduation - PEP, Universidade Tiradentes, 49037-580, Aracaju, SE, Brazil*

[c] *Electrochemistry and Nanotechnology Laboratory, Research and Technology Institute (ITP), Aracaju, SE, Brazil*

[d] *Department of Chemical Engineering, Universidad de Castilla-La Mancha, Campus Universitario s/n, 13071, Ciudad Real, Spain*

* Corresponding authors

manuel.rodrigo@uclm.es (Manuel A. Rodrigo).

marcoslanza@iqsc.usp.br (Marcos Roberto de Vasconcelos Lanza)

Abstract

In this work, it is proposed a novel strategy to increase the photostability of the ZnO photoelectrocatalyst under prolonged light irradiation, without the addition or deposition of metals and/or semiconductor oxides during their synthesis. This strategy is based on the use of a mixed metal oxide (MMO-$Ru_{0.3}Ti_{0.7}O_2$) coating as the substrate for the electrodeposition of ZnO. To assess it, the electrodeposition of ZnO films on Ti and Ti/MMO substrates and the photoelectrocatalytic activity of these materials for the degradation of the herbicide clopyralid were studied. The results showed that the substrate directly influenced the photo-stability of the ZnO film. Under the incidence of UV light and polarization, the novel Ti/MMO/ZnO electrode showed greater photocurrent stability as compared to Ti/ZnO, which is a very important outcome because the behavior of these electrodes was similar when compared in terms of the degradation of clopyralid. Single electrolysis was not able to degrade efficiently clopyralid at the different potentials studied. However, the irradiation of UV light on the polarized surface of the Ti/ZnO and Ti/MMO/ZnO electrodes increased markedly the degradation rate of clopyralid. A synergistic effect was observed between light and electrode polarization, since the rate of degradation of clopyralid was twice as high in photoelectrocatalysis (PhEC) than in photocatalysis (PhC) and different intermediates were formed. From these results, mechanisms of degradation of clopyralid for the PhC and PhEC systems with the Ti/ZnO and Ti/MMO/ZnO electrodes were presented. Therefore, the Ti/MMO/ZnO electrode could be a cheap and simple alternative to be applied in the efficient photodegradation of organic pollutants, presenting the great advantage of having a facile synthesis and high capacity to work at relatively low potentials.

Keywords

electrodeposition; photoanode; photoelectrocatalysis; Ti/ZnO;Ti/MMO/ZnO; clopyralid

Highlights

- Deposition of ZnO on Ti/MMO improves the adhesion and stability of the film
- ZnO deposited on Ti/MMO results in a more porous electrode with large surface area
- Insignificant differences in photoactivity between Ti/ZnO and Ti/MMO/ZnO
- Photoelectrocatalysis present high clopyralid degradation efficiency for both anodes
- Clopyralid oxidation mechanism was dependent on the oxidizing species and UV light

1. Introduction

Pesticides have been widely used worldwide in agriculture to improve the quality and quantity of crops. However, most of these compounds are chemically stable, toxic, non-biodegradable, and resistant to sunlight (Aquino et al., 2017; Souza et al., 2016; Xu et al., 2013). Thus, these substances can be persistent contaminants in the environment, representing a potential risk to the ecosystem and human health. Therefore, several technologies have been used in the degradation of these compounds (Araújo et al., 2015; Brillas, 2014; Llanos et al., 2018; Morillo and Villaverde, 2017).

The advanced oxidative processes (AOP) have stood out due to their high efficiency in the oxidation of recalcitrant organics, associated with the generation *in situ* of oxidizing species such as the hydroxyl radical (Sirés et al., 2014). Among these processes, heterogeneous photocatalytic oxidation has been proven to be effective in degrading a variety of recalcitrant organic compounds. However, the success of this process is directly related to the characteristics of the material used as a photocatalyst (Zhu and Wang, 2017).

ZnO photocatalysts are some of the most attractive semiconductor materials for photocatalytic applications because of their high photosensitivity, high redox potential, low toxicity, high photocatalytic activity, and low cost that is very remarkably when compared to other metallic oxides (Saravanan et al., 2013; Serrà et al., 2019a, 2019b). However, one of the main disadvantages associated with photocatalysis with ZnO is related to the photo-corrosion undergone with the irradiation of light over extended periods (Fu et al., 2008; Zhang et al., 2009). Thus, several research efforts have been made in order to improve the photostability of ZnO throughout its surface modification and doping [2,3]. Another significant factor with a substantial effect on the stability of

ZnO films is the proper immobilization and adhesion of these films to the conductive substrate on which they are deposited (Peleyeju and Arotiba, 2018).

Different methods have been used to obtain ZnO, such as sol-gel, spin-coating (Huang et al., 2017), anodizing (Shetty and Nanda, 2012), spray pyrolysis (Sapkal et al., 2012), electrodeposition (Mahalingam et al., 2005), among others. Electrodeposition has the advantage of being robust, low cost, and is capable of forming uniform and adherent films. Besides, it is possible to obtain different morphologies in the depositing of the films (Dai et al., 2013; Mahalingam et al., 2005). The formation of nanostructures can affect the photocatalytic properties of the material, improving the transport of light for the generation of charge carriers (Cerrón-Calle et al., 2019). The choice of the substrate for electrodeposition is essential because it directly affects the characteristics of the material formed (Stumpp et al., 2018). A highly porous substrate, in addition to having a high surface area, can influence the formation of particularly structured morphologies of the deposited film. In a photocatalyst, these hierarchical structures can improve both the adsorption of pollutants and the ability to capture light, leading to increasing photocatalytic activity of the material (Chou et al., 2007; Serrà et al., 2019a). In this way, the deposition of the ZnO film on a substrate with high electrochemical stability and surface area, such as mixed metal oxide (MMO) films, would be remarkable (Moura de Salles Pupo et al., 2019).

Another disadvantage of the use of ZnO in photocatalysis is its high recombination of photogenerated charges (Mou et al., 2018). Thus, strategies such as the application of external potential can assist in the separation of charges and the formation of oxidizing species, improving the photocatalytic performance of the system. In photoelectrocatalysis (PhEC), the constant polarization of a photoanode under light irradiation and cell potential or constant current density, promotes the extraction of the photo-induced

electron (e^-_{cb}) by the external electrical circuit, leading to an efficient separation of the photogenerated charges (e^-_{cb} / h^+_{vb}) and decreasing its recombination(Garcia-Segura and Brillas, 2017). Therefore, PhEC has been shown to be a more efficient technique in the degradation of organic compounds when compared to photocatalysis (PhC), as there is a synergistic effect between electrochemical processes and light, thus generating more oxidizing species and increasing the time of photo-generated charges (Araújo et al., 2015; Philippidis et al., 2009; Rubí-Juárez et al., 2016).

Taking into account this background, in this work, it has been evaluated the influence of Ti and MMO substrates on the electrodeposition of ZnO coatings and the photoactive stability of the resulting materials at different potentials. Thus, the photoactivity of the Ti/ZnO and Ti/MMO/ZnO photoelectrodes was evaluated based on the degradation of the herbicide clopyralid, used as a model compound, where the effect of light and potential applied were compared, and a degradation mechanism was proposed in order to understand the role of each parameter in the performance of these photoactive electrodes.

2. Experimental

2.1 Chemicals

Clopyralid (99%), titanium (IV) butoxide (97%), ruthenium (II) chloride ($RuCl_3.xH_2O$, 99.9%) and zinc acetate (99%) were purchased from Sigma-Aldrich. Potassium nitrate and anhydrous sodium sulfate were from Panreac. Methanol and HPLC grade formic acid were obtained Sigma-Aldrich. All aqueous solutions were prepared with ultrapure water from a Millipore Mili-Q Gradient system (resistivity 18.2 MΩ cm).

2.2 Ti/ZnO and Ti/MMO/ZnO synthesis

Initially, the titanium substrates (6.25 cm^2 area) were polished with sandpapers of different granulometry and carefully treated in 20% hydrochloric acid solution (HCl, 38.0% from Neon®) and 10% oxalic acid solution (99.5%, from Vetec®) for 15 min each at 80 °C, being finally rinsed with ultrapure water. The acid treatment of the titanium plates is done to remove impurities and the TiO_2 layer formed by the oxidation of the substrate surface in contact with air (Terezo and Pereira, 1999).

The Ti/MMO substrate was obtained from a precursor solution deposited onto a previously treated titanium substrate. The precursor solution of MMO consisted of a mixture of ruthenium chloride and titanium butoxide in a molar ratio of 0.3/0.7 (Ru/Ti) maintained under mechanical stirring until complete dissolution at 80 °C in an ionic liquid (hydrogen sulfate-methylimidazolium) previously described (de Mello et al., 2018). This precursor solution was painted onto the titanium substrate surface until the full coverage of the titanium surface. At each deposited layer, the electrode was calcined for 5 min at 400 °C, with the heating rate of 5 °C min^{-1}. The titanium substrate was weighed before and after each layer of MMO to verify the deposited film mass. Layers of the MMO film were made until the coating reached a mass of 1.2 mg cm^{-2}, where it was calcined for 1 h at 400 °C, thus obtaining the Ti/MMO substrate.

ZnO was formed on the surfaces of Ti and Ti/MMO by electrodeposition and further calcination. For electrodeposition, the Ti and Ti/MMO substrates were submerged in an aqueous solution of 50 mM of zinc acetate in 0.1 M of potassium nitrate. The pH of the solution was adjusted to 5.8 with a 2.0 mM nitric acid solution. The solution was maintained at 80 °C, and the electrodeposition was performed initially on the Ti substrate applying a –1.1 V potential vs. Ag/AgCl (saturated KCl) for different times (5, 10, 20, 30, and 60 min) and 30 min on the Ti/MMO anode. The deposition of ZnO can be

explained by the reaction of the Zn^{2+} ions present in the solution with hydroxide ions formed from the electrochemical reduction (Biswas et al., 2016), according to Eqs. (1–4).

$$NO_3^-{}_{(aq)} + H_2O + 2e^- \rightarrow NO_2^-{}_{(aq)} + 2OH^-{}_{(aq)} \quad (1)$$

$$2H_2O + 2e^- \rightarrow H_2 + 2OH^-{}_{(aq)} \quad (2)$$

$$CH_3COO^-{}_{(aq)} + H_2O \rightarrow CH_3COOH_{(aq)} + OH^-{}_{(aq)} \quad (3)$$

$$Zn^{2+}{}_{(aq)} + 2OH^-{}_{(aq)} \rightarrow Zn(OH)_{2(s)} \rightarrow ZnO_{(s)} + H_2O \quad (4)$$

After the electrodeposition step, the films were washed with ultrapure water and then calcined for 1 h at 400 °C with a heating rate of 5 °C min^{-1}. The calcination temperature of ZnO in Ti also was studied at 500, 600 and 700 °C.

2.3 Electrochemical characterization

The Ti/MMO, Ti/ZnO and Ti/MMO/ZnO electrodes were used as working electrodes, Ag/AgCl (saturated KCl) from Metrohm as the reference electrode, and a Pt plate as a counter electrode in the electrochemical characterizations. The voltammetric profiles of the electrodes were evaluated by linear sweep voltammetry and cyclic voltammetry at a scan rate of 20 mV s^{-1} in an electrochemical cell with a capacity of 150 mL.

Cyclic and linear sweep voltammetry experiments were performed between –0.6 and 1.2 V in 0.1 M Na_2SO_4 solution without and with UV light irradiation, using a UVC lamp (with 254 nm) of 9 W, with photon irradiance (*Ei*; ~ 20 mW cm^{-2}), in order to assess the photoactivity of the ZnO electrodeposited on different substrates. The same lamp was used for all experiments with light irradiation, in order to keep the photon flow constant, since it influences on the photoelectrocatalytic efficiency and photocurrent responses of the anode(Garcia-Segura et al., 2018). The ZnO stability in Ti and Ti/MMO substrates was studied by using chronoamperometry, applying different potentials (i.e., 0.2; 0.5, 0.7; 1.0, and 1.2 V) for 30 min under UV light irradiation. The

stability of the films was monitored by the difference between the initial photocurrent obtained by linear sweep voltammetry under light irradiation and after the application of each potential. All electrochemical measurements were carried out in a potentiostat/galvanostat (Autolab PGSTAT 302N - Metrohm), coupled to a computer-controlled by the NOVA program, version 2.1.

2.4 Physical characterization

The morphology of the films and their elementary composition were obtained by using a field emission scanning electron microscope (FE-SEM; Zeiss GeminiSEM 500) with a coupled energy-dispersive X-ray (EDX) spectroscopy analyzer. The identification of the phases present in the oxide films deposited on Ti was carried out by X-ray diffraction patterns (XRD) taken using a Bruker-D8 Advanced X-ray diffractometer with Cu Kα radiation over a 2 θ range 20 °–80 °; scan rate of 0.02 ° min^{-1}.

2.5 Degradation assays

The Ti/ZnO and Ti/MMO/ZnO electrodes were used as anodes for the degradation of the herbicide clopyralid, molecule presented at the Table 1. The degradation experiments were carried out in the same electrochemical cell used for the photocurrent measurements (system with three electrodes), with the lamp in the center and directly radiating the surface of the anodes. The effect of light and the application of potentials (0.2; 0.5, and 0.7 V) in the degradation of 20 mg L^{-1} of clopyralid in 0.1 M Na_2SO_4 solution for 4 h was evaluated.

Table 1. Some properties of Clopyralid

Characteristics	Clopyralid

Chemical structure	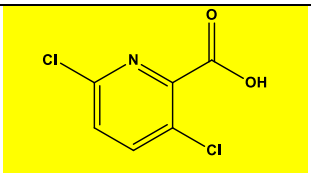
Name	3,6-dichloropyridine-2-carboxylic acid
Molecular weight (g/mol)	192.0

2.6 Analytical techniques

During the degradation experiments, aliquots were collected and filtered using a 0.22 µm filter before analysis. The concentration of clopyralid and the formation of organic intermediates were examined by an HPLC from Agilent 1100, equipped with a diode array detector adjusted to a wavelength of 280 nm and an Eclipse Plus C-18 column (4.6 mm × 100 mm; 3.5 µm). The mobile phase used consisted of a mixture of methanol and water, 30/70 (v/v), the flow was 1.0 mL min^{-1}, the injection volume 20 µL and a temperature of 20 °C. The formation of carboxylic acids was monitored by an HPLC with a ZorbaxSB-Aq column (4.6 mm × 150 mm) and a mobile phase of 5.0 mM H_2SO_4, λ = 210 nm.

3. Results and discussion

3.1 ZnO electrodeposition and photoactivity

The electrodeposition of ZnO was initially carried out on a Ti substrate and the films were calcined at 400 °C. Fig. 1a shows the linear sweep voltammograms obtained with the Ti/ZnO electrodes at different electrodeposition times in a 0.1 M Na_2SO_4 solution without and under lighting. With the incidence of light, the current of the linear sweep voltammograms increases when compared to a Ti/ZnO electrode in the dark, showing that in all conditions studied, the deposition of ZnO took place, which is a photoactive

semiconductor. The photocurrent of the electrodes varied with the deposition time of the ZnO. Insignificant differences in the photocurrent are noted for ZnO films obtained in 5 and 10 min. The intermediate photocurrent densities (around 400 μA cm^{-2}) yielded for these catalysts may be related to the formation of thin ZnO films and some failure in the total coverage of the Ti substrate (Fig. S1). However, an increase in the photocurrent is observed for the electrodes obtained at 20 and 30 min, with values of 700 and 900 μA cm^{-2}, respectively. These films showed greater coverage of the Ti surface. A thicker ZnO film was formed when increasing the deposition time up to 60 min, and a decrease in the photocurrent of the material was observed. This outcome can be explained considering that very thick films can increase the recombination of the photogenerated charges, reducing the photoactivity of the material (Goulart et al., 2019). Another factor that can influence the decrease in photoactivity is an increase in the resistance of the electrodeposited metal oxide layer in longer deposition times. The morphological characterization of all films displayed in the Supplementary Material (Fig. S1), shows how the deposition time influences the amount of the deposited ZnO film.

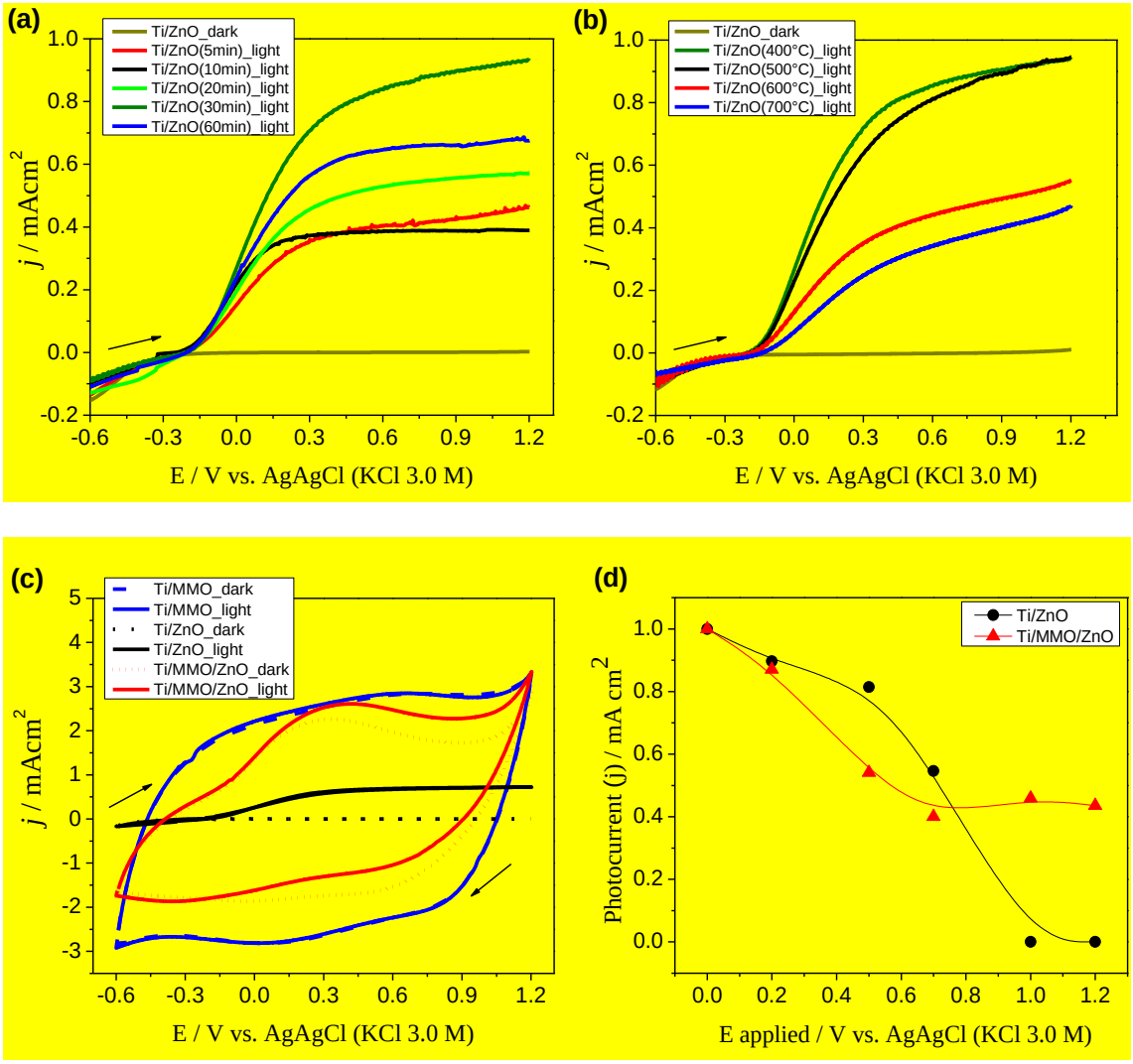

Fig. 1. Linear sweep voltammograms of the Ti/ZnO electrode at different electrodeposition times (5, 10, 20, 30 and 60 min) calcined at 400°C (A) and at different calcination temperatures (400, 500, 600 and 700 °C) electrodeposited at 30 min (B); cyclic voltammograms of the MMO, Ti/ZnO and Ti/MMO/ZnO (C) electrodes; photocurrent behavior of Ti/ZnO (●) and Ti/MMO/ZnO (▲) electrodes applying potentials of 0.2, 0.5, 0.7, 1.0, and 1.2 V for 1800 s (D). All experiments were carried out in a 0.1 M Na_2SO_4 solution without and under irradiation of light.

Another parameter studied in the formation of ZnO was the calcination temperature. Fig. 1b shows the linear sweep voltammograms of the Ti/ZnO electrodes electrodeposited at

30 min and calcined at 400, 500, 600, and 700 °C without and under the incidence of light. The ZnO films obtained at 400 and 500 °C showed similar photocurrent values. However, photoactivation with the incidence of light and the stability of the photocurrent is slightly faster in the electrode obtained at 400 °C than at the calcined at 500 °C. At 400 °C, there is the formation of ZnO films with different particle structures and sizes. The non-uniformity of the particles appears to form a porous film and with high active area. The ZnO film obtained at 500 ° C also has porosity, with the formation of more uniform and aggregated particles compared to obtained at 400 ° C. The porosity of the ZnO films at different calcination temperatures was evaluated using SEM images presented in supplementary material. The increase in the calcination temperature up to 600 and 700 °C decreased the photoactivity of the electrodes. It may be related to the higher aggregation of the ZnO particles and the smaller surface area of the formed films (Fig. S2). The aggregation of particles during calcination can reduce the free available surface of the material, and the growth of the grains decreases the energy of the crystal surface. Increasing the calcination temperature can also shrink pores and cause compact shrinkage (Salavati-Niasari et al., 2009). Thus, the increase particles size due to crystallization, and the collapse of the mesoporous structure resulting from the agglomeration of ZnO particles, leads to a reduction in the surface area of the film (Baharudin, K. B.; Abdullah, N; Derawi, 2018). Therefore, lower photocurrents were produced by the films synthesized by using the highest temperatures (600 and 700 °C). Thus, the electrode calcined at 400 °C was chosen to continue the study.

Then, the deposition of the ZnO film on an MMO substrate was studied using the deposition time of 30 min and calcination at 400 °C. Fig. 1c shows the voltammetric behavior of the Ti/ZnO, Ti/MMO and Ti/MMO/ZnO electrodes without and with the incidence of light in a 0.1 M Na_2SO_4 solution. Cyclic voltammetry (CV) profile of the

Ti/MMO presents behavior typical of this type of electrode, with a wide region of double layer (i. e. pseudocapacitive behavior) in the potential range between the hydrogen evolution reaction (HER) and oxygen (OER) (de Mello et al., 2018; Santos et al., 2020). The photocurrent of the electrodes is measured by the difference between the current obtained by scanning the potential in the dark and under the incidence of light. The Ti/MMO electrode is not photoactive, so the voltammograms obtained in the dark and under light irradiation are similar. However, the ZnO film was successfully electrodeposited onto the Ti/MMO since the capacitive current of the voltammogram decreases, and the electrode is photoactivated under the incidence of light. In addition, the photocurrent observed for the Ti/ZnO and Ti/MMO/ZnO electrodes were quite similar, around 900 μA cm^{-2}, which shows the effectiveness of the ZnO deposition method on the different substrates. The Ti/MMO/ZnO shows a CV profile similar to that found in the Au/ZnO electrode previously reported in the literature (Gao et al., 2018), with a poorly defined cathodic peak around 0.1 V and an anodic peak around 0.2 V attributed to ZnO. In addition, the capacitive behavior of Ti/MMO/ZnO may be assign to a process of electro-adsorption of Na^+ ions in different electroactive locations of the ZnO film ($ZnO + Na^+ + e^- \rightleftharpoons (ZnO)surface^-Na^+$).

One of the main problems of ZnO is its instability in the presence of light and the formation of films that are not very adherent to the substrate. Therefore, the stability of ZnO in metallic titanium and Ti/MMO substrates was studied. Fig. 1d shows the behavior of the photocurrent of the Ti/ZnO and Ti/MMO/ZnO electrodes by applying potentials of 0.2, 0.5, 0.7, 1.0, and 1.2 V in a solution of 0.1 M of Na_2SO_4. The photocurrent of the electrodes decreases with the increase in the potential applied to both electrodes. However, starting at 0.7 V, the photocurrent stabilized for the Ti/MMO/ZnO electrode, which is very important in particular when compared to Ti/ZnO, where the photocurrent

reaches zero at potentials as high as 1.0 and 1.2 V. This behavior shows that on the titanium substrate, the ZnO is less stable, and the potential range in which this electrode is active is narrower. The use of the Ti/MMO substrate, on the other hand, increases the working potential range under the incidence of light. Due to the cracked-mud structure of the MMO film and its higher porosity, the ZnO film is deposited in a larger surface area. Even with the photocorrosion process taking place in the outermost layer of the ZnO film electrodeposited in MMO, the ZnO is adhered to the pores and contours of the MMO particles in the innermost layer of the electrode, maintaining the photoactivity of the material at high potentials. Thus, the deposition of ZnO on a film of a mixture of dimensionally stable oxides improves the adhesion and stability of the photoactive film.

3.2 Structural and morphological characterization

The morphology of the Ti/MMO electrode and the Ti/ZnO and Ti/MMO/ZnO electrodes deposited for 30 min and calcined at 400 °C was evaluated by scanning electron microscopy (SEM). The SEM images in Fig. 2a show that the Ti/MMO has the cracked-mud type morphology typical of films obtained by thermal decomposition (da Silva et al., 2018). The Ti/ZnO electrode image shows the formation of a ZnO film with different particle structures and sizes (Fig. 2b). However, the structure of ZnO changes when it is deposited on the MMO (Fig. 2c). Note the formation of a more porous electrode with smaller particles, which gives a larger surface area.

The measures of energy-dispersive X-ray spectroscopy (EDX) showed the presence of oxygen, titanium, and ruthenium in the Ti/MMO electrode; oxygen, zinc, and titanium in the Ti/ZnO electrode and oxygen, titanium, zinc, and traces of ruthenium in the Ti/MMO/ZnO indicating the good coverage of the MMO film with ZnO. In Fig. 2 (d, e, f), the color mapping images are presented, whereas Fig. 2 (g, h, i) displays the EDX spectra of the Ti/MMO, Ti/ZnO, and Ti/MMO/ZnO electrodes, respectively. Note the

homogeneous dispersion of all the elements detected in the color mapping along the surface of the electrodes.

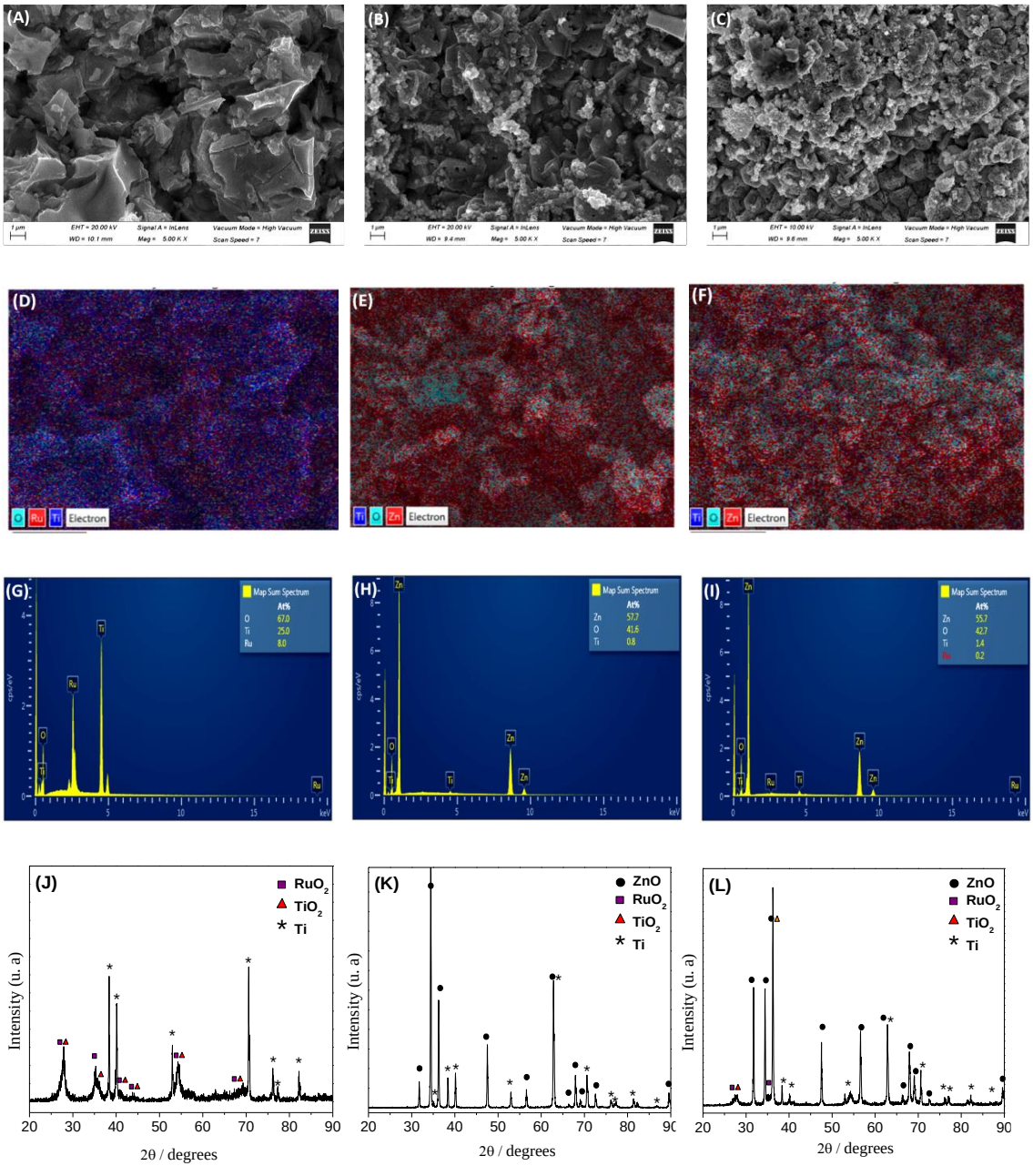

Fig. 2. SEM image, Elemental mapping, EDX spectra and XRD plots of Ti/MMO (A, D, G, and J), Ti/ZnO (B, E, H, and K), Ti/MMO/ZnO (C, F, I, and L). The Ti/ZnO and Ti/MMO/ZnO were obtained with 30 min of electrodeposition and calcinated at 400 °C.

The crystalline structures of the Ti/MMO, Ti/ZnO, and Ti/MMO/ZnO electrodes were evaluated by XRD (Fig. 2j, k, l). RuO_2 was formed in the rutile phase (JCPDS 00-040-1290), while TiO_2 in the anatase (JCPDS 00-00109562) and rutile (00-004-0551) phases in the MMO electrodes. ZnO with hexagonal wurtzite structure (JCPDS 36-1451) was observed in the Ti/ZnO and Ti/MMO/ZnO electrodes. The metallic Ti found in the XRD of the electrodes is corresponding to the X-ray penetration through the titanium substrate (de Mello et al., 2018).

3.3 *Clopyralid degradation*

The photocatalytic activity of the Ti/ZnO and Ti/MMO/ZnO electrodes was evaluated in the degradation of clopyralid under UVC light irradiation and applying potentials of 0.2, 0.5 and 0.7 V in 0.1 M Na_2SO_4 solution for 4 h. The rate of degradation of clopyralid is shown in Fig. 3, where the relative concentration of the molecule decays over 4 h under the different conditions studied. In the electrolysis, no degradation of clopyralid was observed for both electrodes investigated (Fig. S3). This behavior may be related to the low potentials applied during electrolysis, which make it impossible to generate reactive oxygen species responsible for the transformation of clopyralid by direct transfer processes. In addition, photoanodes present relatively low current in the absence of irradiation. However, the light played a fundamental role in the degradation of clopyralid. In the photolysis experiments (only UV light radiation), 18.2% of the molecule was degraded, Fig. 3a. This behavior may be related to the photoactive characteristic of most herbicides. The presence of aromatic rings, heteroatoms, and other functional groups in the structures of these compounds leads to the absorption of UV-vis radiation (direct photolysis) or photodegradation that occur from the reaction with photosensitive species (indirect photolysis) (Orellana-García et al., 2014; Prados-Joya et al., 2011). Although some studies in the literature report the low degradation of clopyralid under irradiation of

UV light (1.4 to 10% of degradation), and associate the results found with the formation of a bicyclic valence isomer (Dewar pyridine) formed under irradiation 254 nm, which it is re-aromatized in a few minutes making the system inefficient(Barbosa Ferreira et al., 2020; Semitsoglou-Tsiapou et al., 2016), in our work, photolysis promoted about 20% degradation. It is important to note that in addition to the structural characteristics of the molecule, several other factors can influence the degradation process by photolysis, such as ultraviolet fluency, the molar absorption coefficient (1044 M^{-1} cm^{-1} for clopyralid) (Semitsoglou-Tsiapou et al., 2016), concentration of molecule, reaction medium, irradiation time, among others (Orellana-García et al., 2014).

About 40% of the clopyralid was degraded in the photocatalysis experiments with the incidence of UVC light on the surface of the Ti/ZnO and Ti/MMO/ZnO electrodes. As the electrodes are made of a ZnO film that is a photoactive semiconductor, the irradiation of UV light promotes the generation of electron/hole pair (e_{cb}^{-}/h_{vb}^{+}). When ZnO is irradiated with light with energy greater than or equal to its energy band gap, the excitation of an e^{-} from the valence band (vb) to the conduction band (cb) occurs, leading to the formation of an h_{vb}^{+}. These photogenerated charges migrate separately to the material surface and react with O_2 and OH^{-} in the solution, leading to the formation of superoxide radical anions ($O_2^{\bullet -}$), hydroxyl radicals ($^{\bullet}OH$) and hydroperoxyl radicals ($^{\bullet}OOH$). Among these species, the hydroxyl radical is the oxidant with the greatest capacity to degrade organic pollutants present on or near to the surface of the catalyst (Stan et al., 2015).

However, the e_{cb}^{-}/h_{vb}^{+} pair usually recombines in the photoactive materials, reducing the formation of oxidizing species, directly influencing the photodegradation process. For this reason, the application of direct polarization on photoactive electrodes is generally used to increase the separation of the photo-generated charges and the efficiency of the

material (Papagiannis et al., 2018). An increase in the percentage of clopyralid degradation was observed in the photoelectrocatalysis experiments for both studied electrodes. The degradation of clopyralid was 71 and 77% in the Ti/ZnO and Ti/MMO/ZnO electrodes, respectively, applying a potential of 0.5 V and UVC light for 4 h (Fig. 3a). Fig. 3b shows the decay of the relative concentration of clopyralid as a function of time in photoelectrolysis performed with potentials 0.2, 0.5, and 0.7 V. It was observed that the polarization of the electrodes was necessary to increase the efficiency of the clopyralid degradation process. At low potentials, 0.2 and 0.5 V, the percentage of clopyralid degradation is very similar, around 77%. However, applying 0.7 V, the degradation of clopyralid decreased down to 60%. The increase in potential promoted a slight decrease in the synergistic effect. Other researchers have also observed this behavior in the photoelectrodegradation of organic compounds (Byrne et al., 2002; Liu et al., 2011; Zhao and Zhu, 2006). When the applied potential exceeds 0.5 V in photoelectrolysis processes, the generation of degradation products on the catalyst surface is facilitated (Chang et al., 2017). These oxidation intermediates formed in the first minutes of photoelectrolysis may have less complex structures and are more susceptible to degradation when compared to clopyralid. Thus, they are preferably oxidized on the surface of the catalyst, inhibiting both the adsorption of the clopyralid on the electrode surface and the rate of degradation.

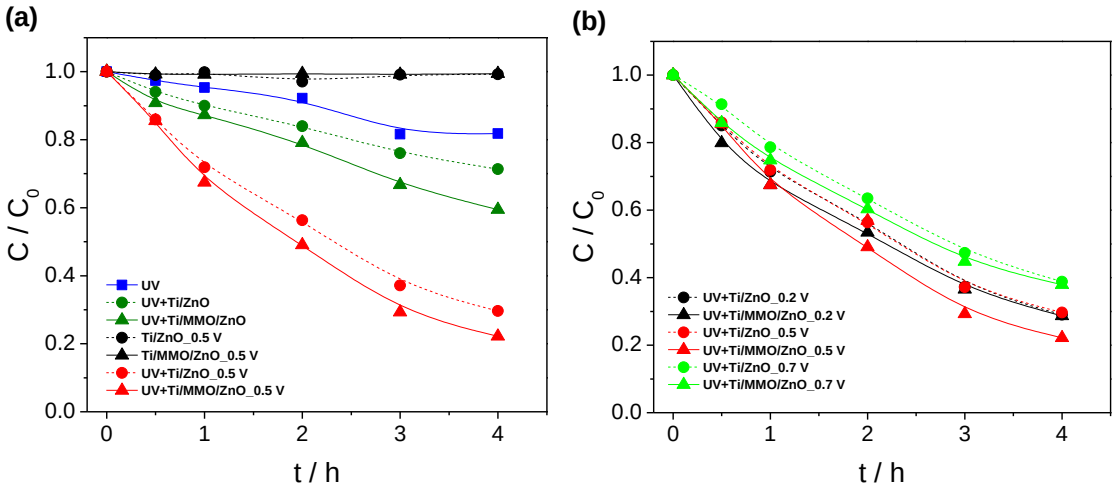

Fig. 3. Effect of photolysis, photocatalysis, electrolysis and photoelectrolysis (a) and photoelectrolysis at different potentials (b) on the degradation of 20 mg L^{-1} clopyralid in 0.1 M Na_2SO_4 with Ti/ZnO (●) and Ti/MMO/ZnO (▲) electrodes.

Fig. 4 shows the constant rates as a function of the polarization potential applied to the Ti/ZnO and Ti/MMO/ZnO electrodes under the incidence of UV light. The apparent degradation rate constants were 0.083, 0.312, 0.309, and 0.242 min^{-1} for Ti/ZnO and 0.127, 0.307, 0.388, and 0.244 min^{-1} for Ti/MMO/ZnO from 0 V to 0.7 V respectively. All the photoelectrolysis rate constants were higher than in the photocatalysis experiments. The rate of degradation of clopyralid increased with increasing potential up to 0.5 V, and a steady rate decline was observed at 0.7 V. However, the rate of degradation at 0.7 V is still about twice that seen in photocatalysis for both the electrodes. The highest coefficient of synergistic effect for the Ti/ZnO electrode was about 3.7 (3.7 = 0.312/0.083) at the 0.2 V potential and for the Ti/MMO/ZnO electrode it was 3.1 (3.1 = 0.388/0.127) at the 0.5 V potential.

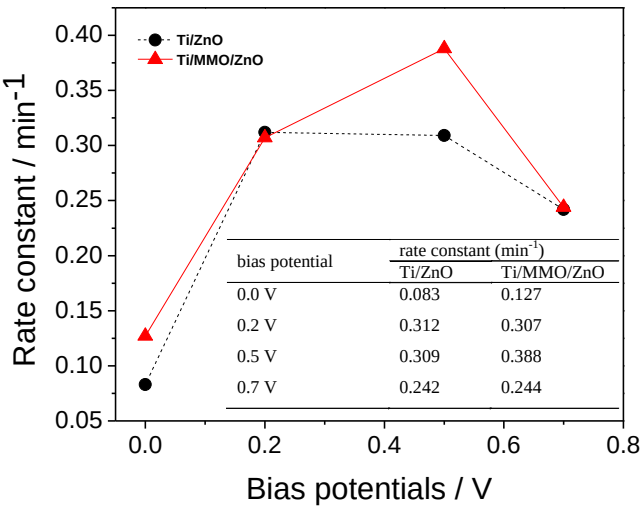

Fig. 4. Dependence of the rate constant on the different polarization potentials for the Ti/ZnO (●) and Ti/MMO/ZnO (▲) electrodes.

The mechanisms of degradation of clopyralid by photocatalysis and photoelectrocatalysis with the Ti/ZnO and Ti/MMO/ZnO electrodes have been proposed.

Regarding the photocatalytic process, with the incidence of light in the ZnO film, the e^-/h^+ pair is generated (Eq. (5)). In the photocatalytic process, the photogenerated holes can directly oxidize the water generating $^{\bullet}OH$ radicals, and the excited electrons react with the O_2 adsorbed on the surface of the electrodes generating $O_2^{\bullet-}$ (Eq. (6) and (7)) (Verbic et al., 2019). All these species attack clopyralid transforming this herbicide into degradation products (Eq. (8)). However, the rate of charge recombination in this system is higher than in photoelectrocatalysis, and this may lead to a decrease in the degradation efficiency of clopyralid (Eq. (9)).

$$ZnO + h\nu \rightarrow e_{cb}^- + h_{vb}^+ \quad (5)$$

$$h_{vb}^+ + OH^- \rightarrow {}^{\bullet}OH \quad (6)$$

$$e_{cb}^- + O_2 \rightarrow O_2^{\bullet-} \quad (7)$$

$$(e_{cb}^- / h_{vb}^+; {}^{\bullet}OH; O_2^{\bullet-}) + \text{Clopyralid} \rightarrow \text{Degradation products} \quad (8)$$

$$h_{vb}^+ + e_{cb}^- \rightarrow \text{recombination of photogenerated loads} \quad (9)$$

During the photoelectrocatalysis, with anodic polarization, the excited electrons from the valence band to the ZnO conduction band are directed to the external circuit to the counter electrode, improving the separation of charges. Meanwhile, the photogenerated holes present on the ZnO surface area available to react with H_2O and form $^{\bullet}OH$ radicals. In addition, the O_2 adsorbed on the surface of the counter electrode can react with the injected electron and the O_2 adsorbed on the surface of the photoactive electrodes (Ti/ZnO and Ti/MMO/ZnO) can react with the photoinduced electrons. Thus, the recombination of charges is reduced, resulting in a greater production of active species, such as $O_2^{\bullet-}$ and $^{\bullet}OH$, improving the rate of clopyralid degradation. The reactions at the anode and cathode in the photoelectrocatalysis are shown in Eqs. (5) to (10).

$$\text{ZnO} + \text{bias potential} \rightarrow \text{external circuit} \qquad (10)$$

As clopyralid proved to be photosensitive, part of its degradation may also occur by the incidence of UV light (Eq. (11)). In addition, the excited electrons from clopyralid can be transferred to the conduction band of ZnO, forming oxidizing species in both photocatalysis and photoelectrocatalysis, according to Eq. (12).

$$\text{Clopyralid} + h\nu \rightarrow \text{Degradation products} \qquad (11)$$

$$\text{Clopyralid} + h\nu \rightarrow \text{Clopyralid}^* \qquad (12)$$

The formation of intermediates was monitored by HPLC. The 2-chloropicolinic acid was identified as the main degradation product in the photolysis, photocatalysis, and photoelectrocatalysis experiments for both electrodes (Fig. 5). In the photoelectrocatalysis performed at 0.2 and 0.5 V, the formation of another unidentified intermediate was also observed but in negligible concentrations. The generation of this new intermediate in the photoelectrocatalysis processes indicates that the coupling of processes can accelerate the fragmentation of the clopyralid.

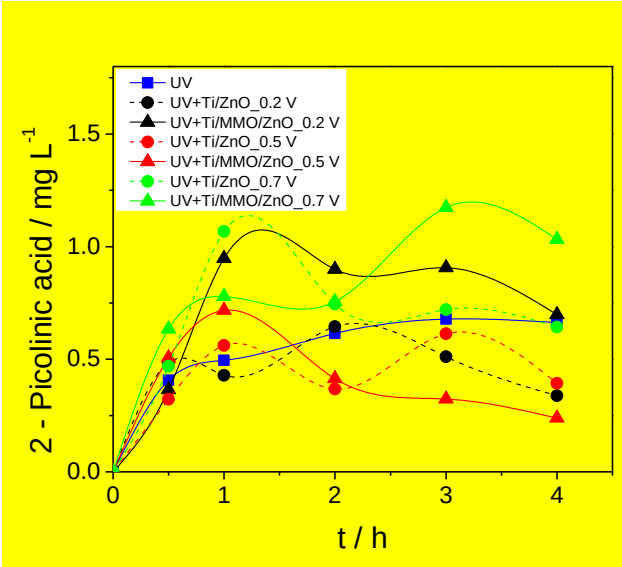

Fig. 5. 2-chloropicolinic acid formed as intermediate during the photolysis, photocatalysis, and photoelectrocatalysis of clopyralid with the Ti/ZnO (●) and Ti/MMO/ZnO (▲) electrodes.

The formation of non-aromatic intermediates was also verified in different potentials for both studied electrodes, including oxalic and oxamic acids in photoelectrolysis and traces of oxamic acid in photolysis, Fig. 6.

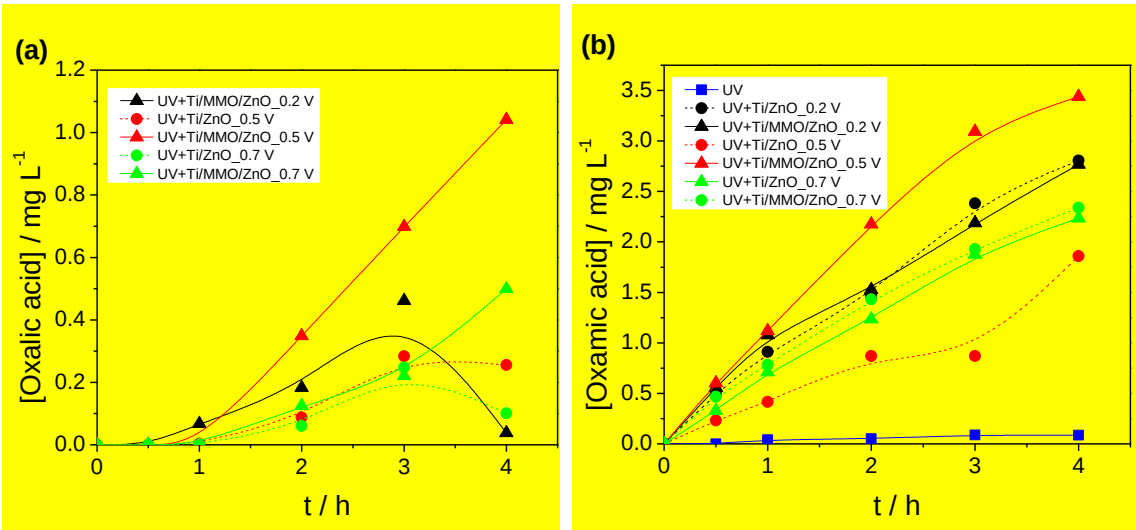

Fig. 6. Carboxylic acids formed in the experiments of photolysis, photocatalysis, and

photoelectrocatalysis of clopyralid with the Ti/ZnO (●) and Ti/MMO/ZnO (▲) electrodes.

Hence, the degradation rate of clopyralid and the intermediate products formed during the photocatalysis and photoelectrolysis processes were very similar using the Ti/ZnO and Ti/MMO/ZnO electrodes. These data show that the ZnO film actually acts in the degradations since insignificant differences in the photoactivity arisen when these films were deposited on titanium or Ti/MMO substrates. However, it was found that the stability of the ZnO film under light and potential is much higher when the Ti/MMO substrate is used as compared to the titanium substrate.

Conclusions

From this work, the following conclusions can be drawn:

- The photocurrents of the Ti/ZnO and Ti/MMO/ZnO electrodes were similar, with the incidence of UV light, showing that in the best conditions of electrodeposition and calcination temperature, Ti and MMO substrates were coated successfully with a ZnO film photoactive;
- The Ti/MMO/ZnO showed the greatest photocurrent stability with the application of external potentials, showing that the substrate can influence on the stability of the deposited ZnO film.

- There was no significant degradation of Clopyralid in the electrolysis experiments for the two studied electrodes since in the photoanodes, the application of the potential generates very low currents in the absence of light.
- Photocatalysis attains the degradation of about 40% of the clopyralid, while photo-electrocatalysis achieves around 77% of degradation at 0.5 V for both electrodes. From these results, a mechanism of oxidation of clopyralid was proposed with oxidizing species formed from the e_{cb}^{-}/h_{vb}^{+} pair and external polarization.

The incidence of light and the polarization of the electrodes were fundamental in the photoactivation and separation of the photo-generated charges of the ZnO film, promoting an increase in the degradation of the clopyralid.

Acknowledgments

Financial support from the Spanish Agencia Estatal de Investigación through projects PID2019-107271RB-I00 and PID2019-110904RB-I00 (AEI/FEDER, UE) is gratefully acknowledged. Financial support by Brazilian research funding agencies is gratefully acknowledged: CNPq (grants no 465571/2014-0, 302874/2017-8, 305438/2018-2, 310572/2016-9 and 427452/2018-0); FAPESP (grants #2014/50945-4, #2016/08760-2, #2019/04084-0 and #2017/10118-0) and CAPES-Finance Code 001.

References

Aquino, J.M., Miwa, D.W., Rodrigo, M.A., Motheo, A.J., 2017. Treatment of actual effluents produced in the manufacturing of atrazine by a photo-electrolytic process. Chemosphere 172, 185–192. https://doi.org/10.1016/j.chemosphere.2016.12.154

Araújo, D.M. De, Cotillas, S., Sáez, C., Cañizares, P., Martínez-Huitle, C.A., Rodrigo,

M.A., 2015. Activation by light irradiation of oxidants electrochemically generated during Rhodamine B elimination. J. Electroanal. Chem. 757, 144–149. https://doi.org/10.1016/j.jelechem.2015.09.025

Baharudin, K. B.; Abdullah, N; Derawi, D., 2018. Effect of Calcination Temperature on the Physicochemical Properties of Zinc Oxide Nanoparticles Synthesized by Coprecipitation. Mater. Res. express 0–7.

Barbosa Ferreira, M., Souza, F.L., Muñoz-Morales, M., Sáez, C., Cañizares, P., Martínez-Huitle, C.A., Rodrigo, M.A., 2020. Clopyralid degradation by AOPs enhanced with zero valent iron. J. Hazard. Mater. 392, 122282. https://doi.org/10.1016/j.jhazmat.2020.122282

Biswas, I., Majumder, M., Roy, P., Mukherjee, D., Chakraborty, A.K., 2016. Nanostructured ZnO thin film with improved optical and electrochemical properties prepared by hydrothermal electrochemical deposition technique. Micro Nano Lett. 11, 351–355. https://doi.org/10.1049/mnl.2015.0528

Brillas, E., 2014. A review on the degradation of organic pollutants in waters by UV photoelectro-fenton and solar photoelectro-fenton. J. Braz. Chem. Soc. 25, 393–417. https://doi.org/10.5935/0103-5053.20130257

Byrne, J.A., Davidson, A., Dunlop, P.S.M., Eggins, B.R., 2002. Water treatment using nano-crystalline TiO2 electrodes. J. Photochem. Photobiol. A Chem. 148, 365–374. https://doi.org/10.1016/S1010-6030(02)00064-3

Cerrón-Calle, G.A., Aranda-Aguirre, A.J., Luyo, C., Garcia-Segura, S., Alarcón, H., 2019. Photoelectrocatalytic decolorization of azo dyes with nano-composite oxide layers of ZnO nanorods decorated with Ag nanoparticles. Chemosphere 219, 296–304. https://doi.org/10.1016/j.chemosphere.2018.12.003

Chang, S., Wang, Q., Liu, B., Sang, Y., Liu, H., 2017. Hierarchical TiO2 nanonetwork-

porous Ti 3D hybrid photocatalysts for continuous-flow photoelectrodegradation of organic pollutants. Catal. Sci. Technol. 7, 524–532. https://doi.org/10.1039/c6cy02150f

Chou, T.P., Zhang, Q., Cao, G., 2007. Effects of Dye Loading Conditions on the Energy Conversion Efficiency of ZnO and TiO2 Dye-Sensitized Solar Cells. J. Phys. Chem. C 111, 18804–18811. https://doi.org/10.1002/chin.200229170

da Silva, L.M., de Oliveira Santiago Santos, G., de Salles Pupo, M.M., Eguiluz, K.I.B., Salazar-Banda, G.R., 2018. Influence of heating rate on the physical and electrochemical properties of mixed metal oxides anodes synthesized by thermal decomposition method applying an ionic liquid. J. Electroanal. Chem. 813, 127–133. https://doi.org/10.1016/j.jelechem.2018.02.026

Dai, S., Li, Y., Du, Z., Carter, K.R., 2013. Electrochemical Deposition of ZnO Hierarchical Nanostructures from Hydrogel Coated Electrodes. J. Electrochem. Soc. 160, D156–D162. https://doi.org/10.1149/2.064304jes

de Mello, R., Santos, L.H.E., Pupo, M.M.S., Eguiluz, K.I.B., Salazar-Banda, G.R., Motheo, A.J., 2018. Alachlor removal performance of Ti/Ru0.3Ti0.7O2 anodes prepared from ionic liquid solution. J. Solid State Electrochem. 22, 1571–1580. https://doi.org/10.1007/s10008-017-3700-6

Fu, H., Xu, T., Zhu, S., Zhu, Y., 2008. Photocorrosion inhibition and enhancement of photocatalytic activity for ZnO via hybridization with C60. Environ. Sci. Technol. 42, 8064–8069. https://doi.org/10.1021/es801484x

Gao, W., Perrot, H., Sel, O., 2018. Tracking the interfacial charge transfer behavior of hydrothermally synthesized ZnO nanostructures: Via complementary electrogravimetric methods. Phys. Chem. Chem. Phys. 20, 27140–27148. https://doi.org/10.1039/c8cp03593h

Garcia-Segura, S., Brillas, E., 2017. Applied photoelectrocatalysis on the degradation of organic pollutants in wastewaters. J. Photochem. Photobiol. C Photochem. Rev. 31, 1–35. https://doi.org/10.1016/j.jphotochemrev.2017.01.005

Garcia-Segura, S., Tugaoen, H.O.N., Hristovski, K., Westerhoff, P., 2018. Photon flux influence on photoelectrochemical water treatment. Electrochem. commun. 87, 63–65. https://doi.org/10.1016/j.elecom.2017.12.026

Goulart, L.A., Alves, S.A., Mascaro, L.H., 2019. Photoelectrochemical degradation of bisphenol A using Cu doped WO 3 electrodes. J. Electroanal. Chem. 839, 123–133. https://doi.org/10.1016/j.jelechem.2019.03.027

Huang, M.C., Lin, J.C., Cheng, S.H., Weng, W.H., 2017. Influence of Ga dopant on photoelectrochemical characteristic of Ga-doped ZnO thin films deposited by sol–gel spin-coating technique. Surf. Interface Anal. 49, 434–440. https://doi.org/10.1002/sia.6176

Liu, Y., Xie, C., Li, H., Chen, H., Liao, Y., Zeng, D., 2011. Low bias photoelectrocatalytic (PEC) performance for organic vapour degradation using TiO2/WO3 nanocomposite. Appl. Catal. B Environ. 102, 157–162. https://doi.org/10.1016/j.apcatb.2010.11.037

Llanos, J., Raschitor, A., Cañizares, P., Rodrigo, M.A., 2018. Exploring the applicability of a combined electrodialysis/electro-oxidation cell for the degradation of 2,4-dichlorophenoxyacetic acid. Electrochim. Acta 269, 415–421. https://doi.org/10.1016/j.electacta.2018.02.153

Mahalingam, T., John, V.S., Raja, M., Su, Y.K., Sebastian, P.J., 2005. Electrodeposition and characterization of transparent ZnO thin films. Sol. Energy Mater. Sol. Cells 88, 227–235. https://doi.org/10.1016/j.solmat.2004.06.021

Morillo, E., Villaverde, J., 2017. Advanced technologies for the remediation of

pesticide-contaminated soils. Sci. Total Environ. 586, 576–597. https://doi.org/10.1016/j.scitotenv.2017.02.020

Mou, H., Song, C., Zhou, Y., Zhang, B., Wang, D., 2018. Design and synthesis of porous Ag/ZnO nanosheets assemblies as super photocatalysts for enhanced visible-light degradation of 4-nitrophenol and hydrogen evolution. Appl. Catal. B Environ. 221, 565–573. https://doi.org/10.1016/j.apcatb.2017.09.061

Moura de Salles Pupo, M., da Silva, L.M., de Oliveira Santiago Santos, G., Barrios Eguiluz, K.I., Salazar-Banda, G.R., 2019. Synthesis and characterization of ternary metallic oxide electrodes containing (SnO2)93Sb5M2 (M = Ce, ta, Bi, Gd) using an ionic liquid as the precursor solvent. Chem. Eng. Commun. 0, 1–19. https://doi.org/10.1080/00986445.2019.1680367

Orellana-García, F., Álvarez, M.A., López-Ramón, V., Rivera-Utrilla, J., Sánchez-Polo, M., Mota, A.J., 2014. Photodegradation of herbicides with different chemical natures in aqueous solution by ultraviolet radiation. Effects of operational variables and solution chemistry. Chem. Eng. J. 255, 307–315. https://doi.org/10.1016/j.cej.2014.06.047

Papagiannis, I., Koutsikou, G., Frontistis, Z., Konstantinou, I., Avgouropoulos, G., Mantzavinos, D., Lianos, P., 2018. Photoelectrocatalytic vs. photocatalytic degradation of organic water born pollutants. Catalysts 8, 1–10. https://doi.org/10.3390/catal8100455

Peleyeju, M.G., Arotiba, O.A., 2018. Recent trend in visible-light photoelectrocatalytic systems for degradation of organic contaminants in water/wastewater. Environ. Sci. Water Res. Technol. 1–45. https://doi.org/10.1039/C8EW00276B

Philippidis, N., Sotiropoulos, S., Efstathiou, A., Poulios, I., 2009. Photoelectrocatalytic degradation of the insecticide imidacloprid using TiO2/Ti electrodes. J.

Photochem. Photobiol. A Chem. 204, 129–136. https://doi.org/10.1016/j.jphotochem.2009.03.007

Prados-Joya, G., Sánchez-Polo, M., Rivera-Utrilla, J., Ferro-garcía, M., 2011. Photodegradation of the antibiotics nitroimidazoles in aqueous solution by ultraviolet radiation. Water Res. 45, 393–403. https://doi.org/10.1016/j.watres.2010.08.015

Rubí-Juárez, H., Cotillas, S., Sáez, C., Cañizares, P., Barrera-Díaz, C., Rodrigo, M.A., 2016. Use of conductive diamond photo-electrochemical oxidation for the removal of pesticide glyphosate. Sep. Purif. Technol. 167, 127–135. https://doi.org/10.1016/j.seppur.2016.04.048

Salavati-Niasari, M., Mir, N., Davar, F., 2009. ZnO nanotriangles: Synthesis, characterization and optical properties. J. Alloys Compd. 476, 908–912. https://doi.org/10.1016/j.jallcom.2008.09.196

Santos, G.O.S., Eguiluz, K.I.B., Salazar-Banda, G.R., Saez, C., Rodrigo, M.A., 2020. Photoelectrolysis of clopyralid wastes with a novel laser-prepared MMO-RuO2TiO2 anode. Chemosphere 244, 125455. https://doi.org/10.1016/j.chemosphere.2019.125455

Sapkal, R.T., Shinde, S.S., Mahadik, M.A., Mohite, V.S., Waghmode, T.R., Govindwar, S.P., Rajpure, K.Y., Bhosale, C.H., 2012. Photoelectrocatalytic decolorization and degradation of textile effluent using ZnO thin films. J. Photochem. Photobiol. B Biol. 114, 102–107. https://doi.org/10.1016/j.jphotobiol.2012.05.016

Saravanan, R., Karthikeyan, S., Gupta, V.K., Sekaran, G., Narayanan, V., Stephen, A., 2013. Enhanced photocatalytic activity of ZnO/CuO nanocomposite for the degradation of textile dye on visible light illumination. Mater. Sci. Eng. C 33, 91–98. https://doi.org/10.1016/j.msec.2012.08.011

Semitsoglou-Tsiapou, S., Templeton, M.R., Graham, N.J.D., Hernández Leal, L., Martijn, B.J., Royce, A., Kruithof, J.C., 2016. Low pressure UV/H2O2 treatment for the degradation of the pesticides metaldehyde, clopyralid and mecoprop - Kinetics and reaction product formation. Water Res. 91, 285–294. https://doi.org/10.1016/j.watres.2016.01.017

Serrà, A., Gómez, E., Philippe, L., 2019a. Bioinspired ZnO-based solar photocatalysts for the efficient decontamination of persistent organic pollutants and hexavalent chromium in wastewater. Catalysts 9, 1–16. https://doi.org/10.3390/catal9120974

Serrà, A., Zhang, Y., Sepúlveda, B., Gómez, E., Nogués, J., Michler, J., Philippe, L., 2019b. Highly active ZnO-based biomimetic fern-like microleaves for photocatalytic water decontamination using sunlight. Appl. Catal. B Environ. 248, 129–146. https://doi.org/10.1016/j.apcatb.2019.02.017

Shetty, A., Nanda, K.K., 2012. Synthesis of zinc oxide porous structures by anodization with water as an electrolyte. Appl. Phys. A Mater. Sci. Process. 109, 151–157. https://doi.org/10.1007/s00339-012-7023-2

Sirés, I., Brillas, E., Oturan, M.A., Rodrigo, M.A., Panizza, M., 2014. Electrochemical advanced oxidation processes: Today and tomorrow. A review. Environ. Sci. Pollut. Res. 21, 8336–8367. https://doi.org/10.1007/s11356-014-2783-1

Souza, F.L., Saéz, C., Lanza, M.R.V., Cañizares, P., Rodrigo, M.A., 2016. Removal of pesticide 2,4-D by conductive-diamond photoelectrochemical oxidation. Appl. Catal. B Environ. 180, 733–739. https://doi.org/10.1016/j.apcatb.2015.07.038

Stan, M., Popa, A., Toloman, D., Dehelean, A., Lung, I., Katona, G., 2015. Enhanced photocatalytic degradation properties of zinc oxide nanoparticles synthesized by using plant extracts. Mater. Sci. Semicond. Process. 39, 23–29. https://doi.org/10.1016/j.mssp.2015.04.038

Stumpp, M., Damtew, D., Stock, D., Hess, K., Schröder, D., Schlettwein, D., 2018. Controlled Electrodeposition of Zinc Oxide on Conductive Meshes and Foams Enabling Its Use as Secondary Anode. J. Electrochem. Soc. 165, D461–D466. https://doi.org/10.1149/2.0941810jes

Subash, B., Krishnakumar, B., Swaminathan, M., Shanthi, M., 2012. Highly efficient , solar active and reusable photocatalyst , Zr loaded Ag-ZnO for Reactive Red 120 dye degradation with synergistic effect and dye sensitized mechanism Highly efficient , solar active and reusable photocatalyst , Zr loaded Ag-ZnO for React. https://doi.org/10.1021/la303842c

Terezo, A.J., Pereira, E.C., 1999. Preparation and characterization of Ti/RuO2-Nb2O5 electrodes obtained by polymeric precursor method. Electrochim. Acta 44, 4507–4513. https://doi.org/10.1016/S0013-4686(99)00182-6

Verbic, A., Gorjanc, M., Simonic, B., 2019. Zinc Oxide for Functional Textile Coatings : Recent Advances. Coatings 9, 1–26.

Xu, G., Liu, N., Wu, M., Bu, T., Zheng, M., 2013. The photodegradation of clopyralid in aqueous solutions: Effects of light sources and water constituents. Ind. Eng. Chem. Res. 52, 9770–9774. https://doi.org/10.1021/ie302844v

Zhang, H., Zong, R., Zhu, Y., 2009. Photocorrosion inhibition and photoactivity enhancement for zinc oxide via hybridization with monolayer polyaniline. J. Phys. Chem. C 113, 4605–4611. https://doi.org/10.1021/jp810748u

Zhao, X., Zhu, Y., 2006. Synergetic degradation of rhodamine B at a porous ZnWO4 film electrode by combined electro-oxidation and photocatalysis. Environ. Sci. Technol. 40, 3367–3372. https://doi.org/10.1021/es052029e

Zhu, S., Wang, D., 2017. Photocatalysis: Basic principles, diverse forms of implementations and emerging scientific opportunities. Adv. Energy Mater. 7, 1–

24. https://doi.org/10.1002/aenm.201700841

Supplementary Material for the paper

Towards a higher photostability of ZnO photo-electrocatalysts in the degradation of organics by using MMO substrates

Lorena A. Goulart[a,d], Géssica O. S. Santos[b,d], Katlin I.B. Eguiluz[b,c], Giancarlo R. Salazar-Banda[b,c], Marcos R. V. Lanza[a,*], Cristina Saez[d], Manuel A. Rodrigo[d *]

[a] *Institute of Chemistry - São Carlos, University of São Paulo, P.O. Box 780, CEP-13560-970 São Carlos, SP, Brazil*

[b] *Processes Engineering Post-graduation - PEP, Universidade Tiradentes, 49037-580, Aracaju, SE, Brazil*

[c] *Electrochemistry and Nanotechnology Laboratory, Research and Technology Institute (ITP), Aracaju, SE, Brazil*

[d] *Department of Chemical Engineering, Universidad de Castilla-La Mancha, Campus Universitario s/n, 13071, Ciudad Real, Spain*

* Corresponding author.

E-mail address: manuel.rodrigo@uclm.es (Manuel A. Rodrigo). marcoslanza@iqsc.usp.br (Marcos Roberto de Vasconcelos Lanza)

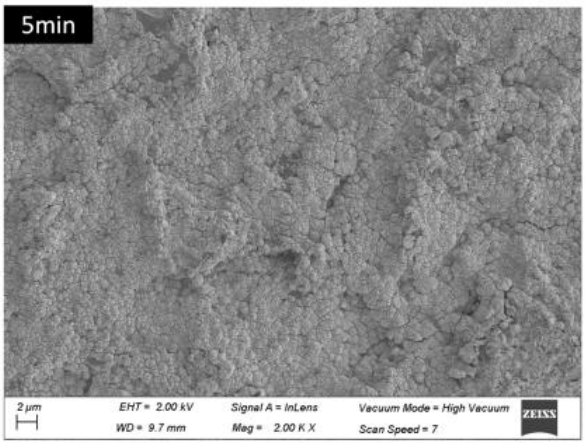
5min
2 µm
EHT = 2.00 kV
WD = 9.7 mm
Signal A = InLens
Mag = 2.00 K X
Vacuum Mode = High Vacuum
Scan Speed = 7
ZEISS

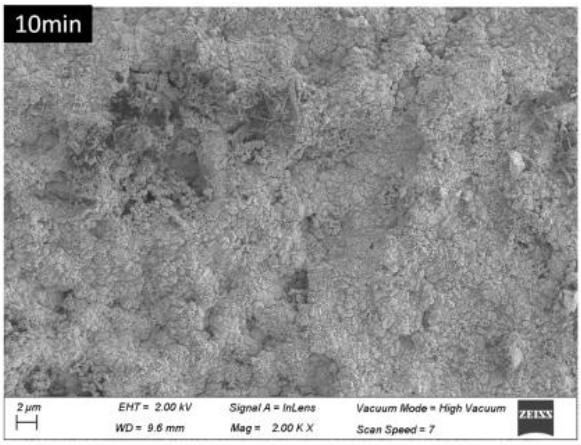
10min
2 µm
EHT = 2.00 kV
WD = 9.6 mm
Signal A = InLens
Mag = 2.00 K X
Vacuum Mode = High Vacuum
Scan Speed = 7
ZEISS

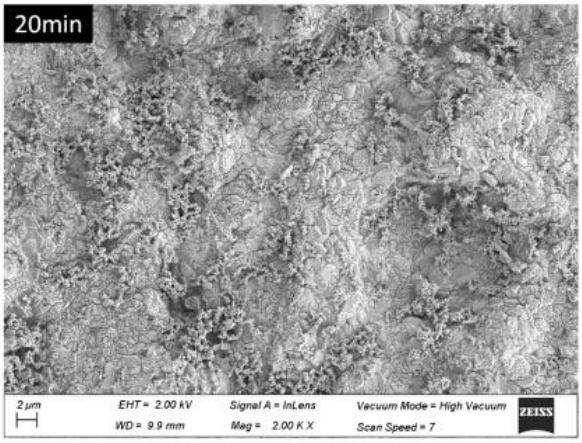
20min
2 µm
EHT = 2.00 kV
WD = 9.9 mm
Signal A = InLens
Mag = 2.00 K X
Vacuum Mode = High Vacuum
Scan Speed = 7
ZEISS

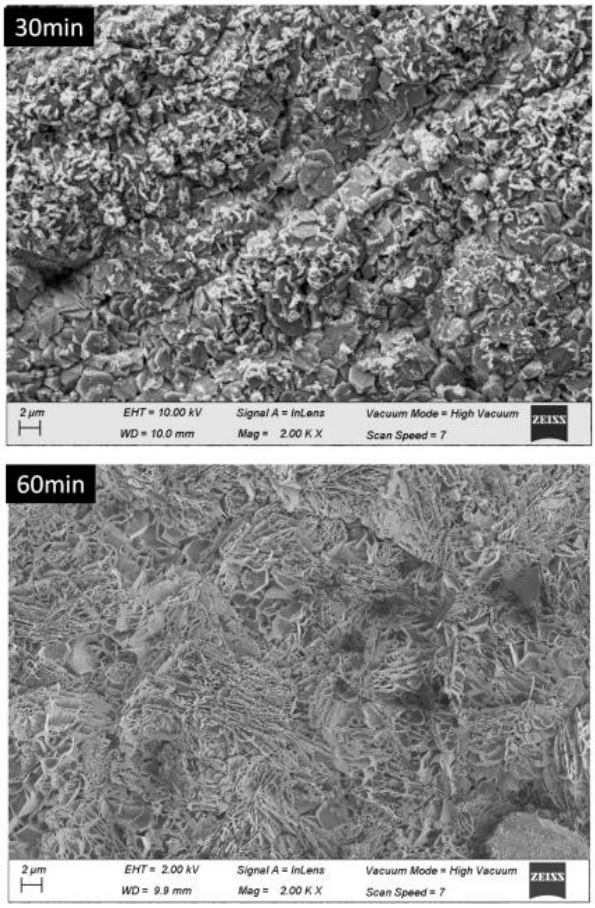

Fig. S1. SEM images of the Ti/ZnO electrodes obtained at different electrodeposition times (5, 10, 20, 30, and 60 min).

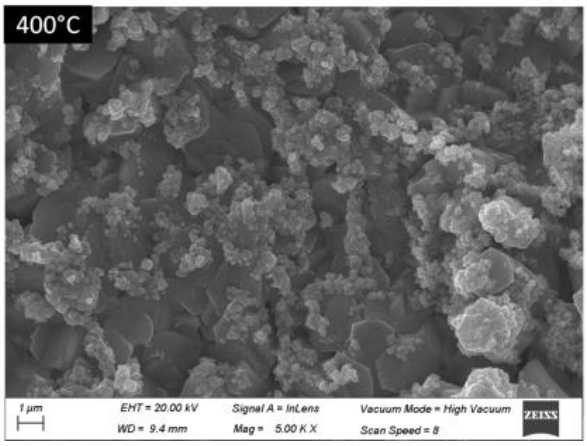
400°C
1 µm
EHT = 20.00 kV
WD = 9.4 mm
Signal A = InLens
Mag = 5.00 K X
Vacuum Mode = High Vacuum
Scan Speed = 8
ZEISS

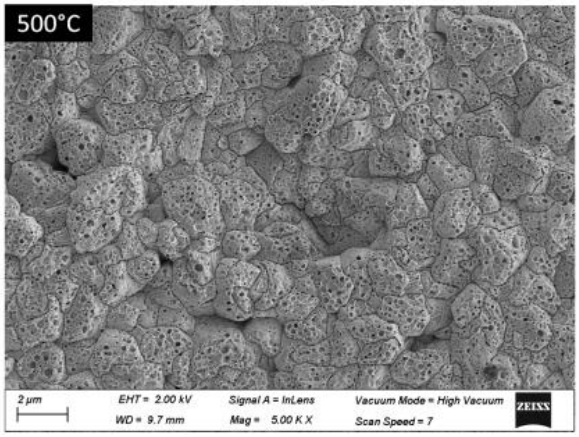
500°C
2 µm
EHT = 2.00 kV
WD = 9.7 mm
Signal A = InLens
Mag = 5.00 K X
Vacuum Mode = High Vacuum
Scan Speed = 7
ZEISS

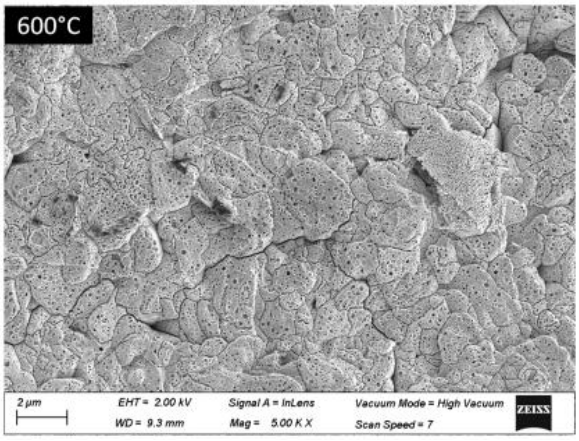
600°C
2 µm
EHT = 2.00 kV
WD = 9.3 mm
Signal A = InLens
Mag = 5.00 K X
Vacuum Mode = High Vacuum
Scan Speed = 7
ZEISS

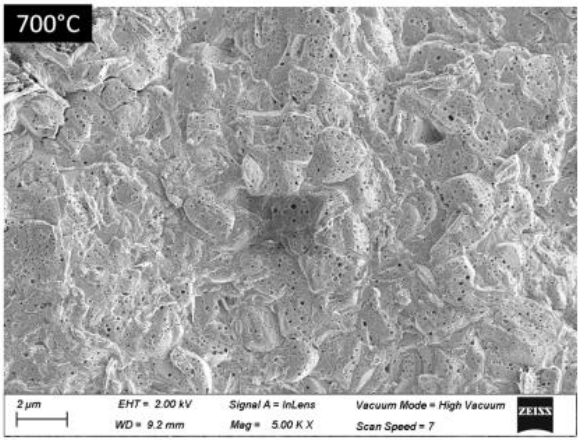
700°C
2 µm
EHT = 2.00 kV
WD = 9.2 mm
Signal A = InLens
Mag = 5.00 K X
Vacuum Mode = High Vacuum
Scan Speed = 7
ZEISS

Fig. S2. SEM images of the Ti/ZnO electrodes synthesized using different calcination temperatures (400, 500, 600, and 700 ° C).

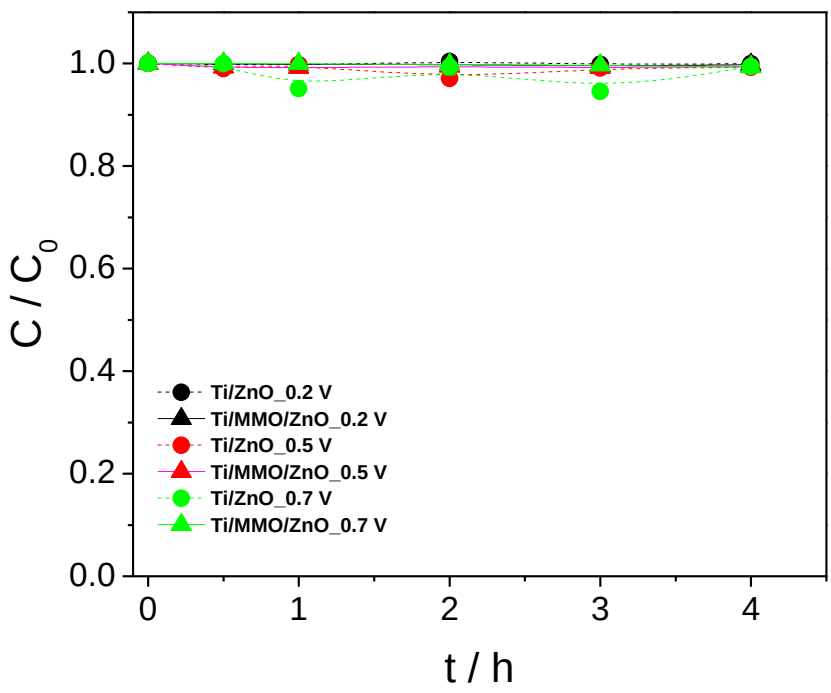

Fig. S3. Effect of the potential on the degradation of 20 mg L^{-1} clopyralid in 0.1 M Na_2SO_4 with the Ti/ZnO and Ti/MMO/ZnO electrodes.